Japanese Journal of Radiology (2025) 43:164–176
https://doi.org/10.1007/s11604-024-01668-3

INVITED REVIEW

Applications of artificial intelligence in interventional oncology: An up-to-date review of the literature

Yusuke Matsui[1] · Daiju Ueda[2] · Shohei Fujita[3] · Yasutaka Fushimi[4] · Takahiro Tsuboyama[5] · Koji Kamagata[6] · Rintaro Ito[7] · Masahiro Yanagawa[8] · Akira Yamada[9] · Mariko Kawamura[7] · Takeshi Nakaura[10] · Noriyuki Fujima[11] · Taiki Nozaki[12] · Fuminari Tatsugami[13] · Tomoyuki Fujioka[14] · Kenji Hirata[15] · Shinji Naganawa[7]

Received: 20 August 2024 / Accepted: 23 September 2024 / Published online: 2 October 2024

Abstract

Interventional oncology provides image-guided therapies, including transarterial tumor embolization and percutaneous tumor ablation, for malignant tumors in a minimally invasive manner. As in other medical fields, the application of artificial intelligence (AI) in interventional oncology has garnered significant attention. This narrative review describes the current state of AI applications in interventional oncology based on recent literature. A literature search revealed a rapid increase in the number of studies relevant to this topic recently. Investigators have attempted to use AI for various tasks, including automatic segmentation of organs, tumors, and treatment areas; treatment simulation; improvement of intraprocedural image quality; prediction of treatment outcomes; and detection of post-treatment recurrence. Among these, the AI-based prediction of treatment outcomes has been the most studied. Various deep and conventional machine learning algorithms have been proposed for these tasks. Radiomics has often been incorporated into prediction and detection models. Current literature suggests that AI is potentially useful in various aspects of interventional oncology, from treatment planning to post-treatment follow-up. However, most AI-based methods discussed in this review are still at the research stage, and few have been implemented in clinical practice. To achieve widespread adoption of AI technologies in interventional oncology procedures, further research on their reliability and clinical utility is necessary. Nevertheless, considering the rapid research progress in this field, various AI technologies will be integrated into interventional oncology practices in the near future.

Keywords Artificial intelligence · Machine learning · Interventional radiology · Oncology · Embolization · Ablation

Introduction

The applications of artificial intelligence (AI) in medicine are rapidly advancing and becoming widespread. The field of radiology is considered particularly well suited for incorporating AI technologies because of the high image-processing capabilities of current AI models. AI has been applied to various aspects of diagnostic radiology and nuclear medicine across various imaging modalities and target organs [1–6]. Studies have shown that AI can be useful for lesion detection [7–10], differential diagnosis [11–15], and image quality improvement [16–21]. Furthermore, the application of AI has been increasingly reported in the field of radiation therapy, where it is used to support various tasks during treatment, including preparation, delivery, and evaluation [22].

The application of AI is being explored also in interventional radiology, a specialty that offers image-guided, minimally invasive therapies [23, 24]. The literature has shown the potential of AI-based tools for intraprocedural support and pre/post-procedural assessment in various interventional radiology fields, including neurointervention, aortic and peripheral vascular intervention, and coronary intervention [25, 26]. Interventional oncology, a subspecialty of interventional radiology, offers image-guided interventions for malignant tumors, with AI-based technologies expected to play a significant role. The key treatments in interventional oncology include transarterial tumor embolization and percutaneous tumor ablation for lesions in various organs [27–32]. In these treatments, imaging is crucial at every stage, from deciding on treatment indications to planning, performing procedures, and post-treatment follow-up. Consequently, interventional oncology may potentially benefit from rapid advancements in AI-based image-processing

Extended author information available on the last page of the article

technologies, leading to significant interest and an increase in relevant studies. This review outlines the current research on AI applications in interventional oncology based on the latest literature.

Overview of literature

A literature search was conducted for this narrative review in June 2024, using PubMed with the following terms: "artificial intelligence," "machine learning," "deep learning," or "neural network," and "interventional oncology," "tumor ablation," "radiofrequency ablation," "microwave ablation," "cryoablation," "embolization," "chemoembolization," or "radioembolization." Notably, 90% (332/371) of the articles identified in the search were published in 2020 or later, indicating a recent rapid increase in research on this topic. We screened these articles and extracted relevant studies for review, primarily focusing on those associated with the clinical application of AI in interventional oncology and excluding those that solely employed animal experimental data or focused on AI methodologies. Additionally, we reviewed several relevant articles found through a manual search of the citations in the reviewed articles or through personal communication.

In the reviewed studies, the application of AI has been attempted in various tasks, including automatic segmentation of organs, tumors, and treatment areas; treatment simulation; improvement of intraprocedural image quality; prediction of treatment outcomes; and detection of post-treatment recurrence (Fig. 1). Among these, the prediction of treatment outcomes has been the most studied. From a technical perspective, the investigators have used deep and conventional machine learning, sometimes comparing these approaches. Here, "conventional machine learning" refers to the machine learning algorithms that have been widely used since the time before the rise of deep learning, including logistic regression, support vector machine, and random forest [33, 34]. These algorithms make decisions using specific functions based on manually selected and engineered features. Deep learning, a subset of machine learning, is based on neural networks, particularly those with multiple layers (33). Deep learning models automatically extract and learn features from data to make decisions with minimal human intervention. In addition, investigators often incorporate machine learning techniques into the radiomics process. Radiomics involves extracting numerous quantitative features that are invisible to the human eye from medical images, which are then analyzed and used to construct models for disease diagnosis, treatment evaluation, and prognostication [35]. In the following sections, we describe how these AI technologies can be applied to interventional oncology based on the literature.

Automatic segmentation of organs, tumors, and treatment areas

AI can potentially enable automatic segmentation of organs, tumors, and treatment areas in interventional procedures, which may contribute to precise tumor targeting, objective evaluation of treatment areas, and potentially lead to a streamlined procedural workflow. Accordingly, some investigators developed AI-based automatic segmentation algorithms using data from patients undergoing image-guided tumor ablation. He et al. investigated a deep learning-based method for segmenting the liver, tumor, and ablation zone using computed tomography (CT) before and after ablation therapy [36]. They trained a residual attention U-net (a U-shaped fully convolutional neural network [CNN]) model using the public dataset of the Liver Tumor Segmentation Challenge (LiTS) [37] and their local dataset of 48 patients who underwent radiofrequency ablation (RFA) or microwave ablation (MWA) for liver tumors. In the test set, their

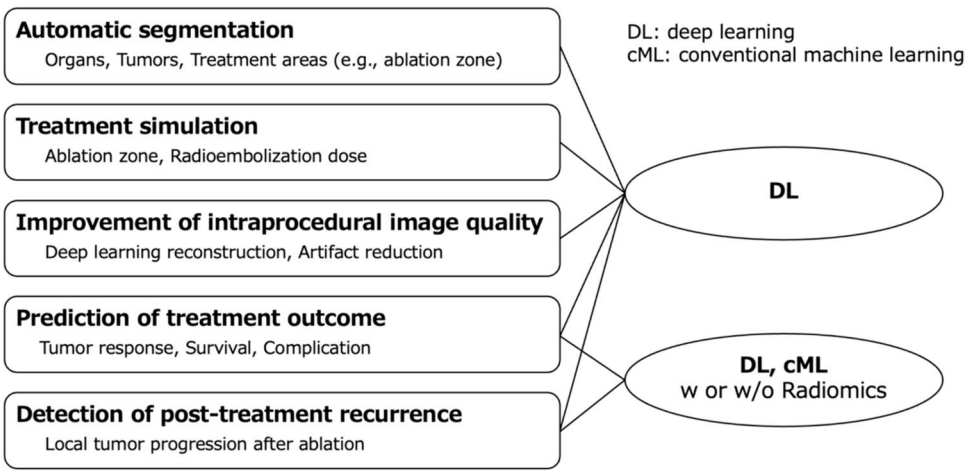

Fig. 1 Application of artificial intelligence in interventional oncology. Deep learning could be utilized for the various tasks mentioned in this review. For outcome prediction and recurrence detection, deep learning or conventional machine learning, with or without radiomics, could be employed

model achieved dice similarity coefficients (DSC) of 0.96, 0.64, and 0.83 for liver, tumor, and ablation zone segmentation in the arterial phase images, where a DSC score closer to 1 indicates a higher overlap between the predicted and true segments. Fang et al. also developed a deep learning-based liver segmentation algorithm using the LiTS dataset and demonstrated that the segmentation method was useful for surface-based image fusion of intraprocedural CT and preprocedural magnetic resonance imaging (MRI), contrast-enhanced CT, or positron emission tomography (PET)/CT images to facilitate tumor targeting [38]. Similar automatic segmentation methods for lung-tumor ablation have been investigated. Mahmoodian et al. developed U-Net-based segmentation models using CT data obtained during CT-guided lung MWA in 50 patients [39]. In their best model, the intersection over union (IoU) values for lung, ablated tissue, and tumor segmentation were 0.98, 0.77, and 0.54, respectively. Here, the IoU was calculated as the area of overlap between the predicted and true segmentations divided by the area of their union, and an IoU value closer to 1 indicates a higher degree of overlap between the segments [40, 41]. Zhou et al. evaluated a U-net algorithm for lung nodule segmentation on preprocedural CT in 55 patients who underwent RFA and obtained DSC and IoU values of 0.88 and 0.88, respectively [42].

Deep learning-based segmentation methods may also be useful for transarterial treatments. Malpani et al. developed a U-net model for the segmentation of lipiodol deposition on cone-beam CT after transarterial chemoembolization (TACE) of liver tumors and compared it to a thresholding method (a method that delineates the lipiodol deposition area based on CT value thresholds) [43]. The U-net model performed better than the thresholding method (DSC; 0.65 vs. 0.45, $p < 0.001$) when segmentation by an experienced radiologist was used as the ground truth. The difference between the predicted and actual center of mass was smaller with the U-net model than with the thresholding method (15.31 mm vs. 31.34 mm, $p < 0.001$), indicating the higher accuracy of the U-net model. Chaichana et al. developed a CNN-based model for the automated segmentation of the lung, liver, and tumors on technetium-99 macroaggregated albumin (^{99m}Tc-MAA) single-photon emission CT (SPECT)/CT images for planning yttrium-90 (^{90}Y) radioembolization of liver tumors [44]. The authors trained the model using images from 56 patients with hepatocellular carcinoma (HCC), which showed DSC of 0.98, 0.91, and 0.85 in the segmentation of lungs, liver, and tumors, respectively, in the test sets. In ^{90}Y radioembolization, accurate segmentation of targets and organs at risk on pretreatment ^{99m}Tc-MAA SPECT/CT is pivotal for precisely predicting microsphere distribution and dose estimation. As segmentation is usually performed manually and is time-consuming, AI-based methods could be of great help in this task.

Treatment simulation

A robust simulation of technical results is crucial for optimizing treatment methods when planning interventional oncology procedures. Some investigators are exploring deep learning-based simulation for image-guided tumor ablation and transarterial radioembolization.

Simulation of ablation zone in ablative therapies

Covering the target tumor with an adequate margin in the ablation zone is necessary to ensure local control during image-guided tumor ablation. The position of the ablation probe is carefully planned before the procedure to achieve an appropriate ablation zone, usually using the vendor's chart for the expected ablation-zone dimensions. However, these vendor data, based on ex vivo animal experiments, often differ significantly from actual patient results because of various factors, such as the local anatomy of each case. For instance, nearby blood vessels can affect heat-based ablation by causing a heat-sink effect [45] or cryoablation by causing a cold-sink effect [46], resulting in narrower ablation zones. Therefore, to accurately predict the ablation zone before the procedure, some investigators have turned to deep learning methods. Keshavamurthy et al. introduced a deep learning model that predicts the ablation zones of lung MWA based on preprocedural CT images, ablation power and time, and applicator position [47]. Data from 52 ablation procedures performed on 40 patients were used and the ablation zones manually segmented on post-treatment images by an experienced radiologist served as the ground truth. Their model outperformed the vendor model (expected ablation zones based on the vendor data) in predicting the ablation zone in the test set (DSC: 0.62 vs. 0.56). Notably, their model could simulate the deformation of the ablation zone caused by the heat-sink effect of blood vessels and the marginal shape along organ boundaries. Moreira et al. reported a deep learning model based on a 3D U-net to predict the ablation zone in cryoablation (iceball) from the position of cryoprobes [48]. The model was trained using the intraprocedural MRI of 38 patients undergoing cryoablation for prostate cancer and predicted the extent of the iceball more accurately than that by the vendor model (DSC: 0.79 vs. 0.72, $p < 0.001$). There was no significant difference between the iceball volume predicted by the model and the ground truth, whereas the volume predicted by the vendor model was significantly smaller than that of the ground truth.

Simulation of absorbed dose in radioembolization

When calculating the expected absorbed doses in ^{90}Y radioembolization therapy, the dose estimation model assumes that the biodistribution of ^{90}Y microspheres in the areas of interest is uniform. However, the estimated absorbed dose based on pretreatment ^{99m}Tc-MAA SPECT/CT often differs significantly from that calculated based on the actual biodistribution of ^{90}Y microspheres confirmed by post-treatment PET/CT or SPECT/CT [49]. Inaccurate absorbed-dose estimation may cause erroneous predictions of treatment response, highlighting the need for more accurate pretreatment dose estimation methods. To address this, Plachouris et al. developed a deep learning model that could generate predicted post-treatment ^{90}Y PET/CT images based on pretreatment ^{99m}Tc-MAA SPECT/CT data to simulate ^{90}Y microspheres biodistribution [50]. Their model, a conditional generative adversarial network (GAN) designed for image-to-image translation, was trained using data from 19 patients undergoing radioembolization for primary or metastatic liver tumors, and its performance was evaluated by comparing image-based dosimetry between the predicted and actual PET-CT images. The difference between the mean absorbed dose calculated on the predicted PET-CT and that on the actual PET-CT was 7.98 ± 31.39 Gy and 0.03 ± 0.25 Gy for the tumor and non-tumoral liver, respectively, suggesting that their deep learning method provided more accurate dose prediction than that by existing methods.

Improvement of intraprocedural image quality

The application of AI to improve medical image quality has been extensively investigated and is being increasingly implemented in clinical practice. Deep learning reconstruction (DLR) of CT and MRI images is representative and can reduce image noise more effectively than traditional reconstruction methods [16–20]. Tanahashi et al. recently explored the use of DLR in interventional imaging, specifically in CT hepatic arteriography images acquired during TACE for HCC [51]. They quantitatively and qualitatively assessed CT hepatic arteriography images of 27 patients using hybrid-iterative reconstruction and DLR techniques and found that DLR improved the signal-to-noise ratio of small hepatic arteries, contrast-to-noise ratio of tumors, and visualization of tumor-feeding arteries. DLR may also reduce radiation exposure in CT-guided procedures, as it can ensure adequate image quality even with lower radiation doses than those in conventional reconstruction techniques. Matsumoto et al. investigated the radiation dose during CT-guided biopsies and drainage using a 320-detector row CT with DLR and reported that using this system significantly lowered radiation doses compared to conventional CT systems (dose length product: 278 vs. 548 mGy*cm in biopsies and 246 vs. 667 mGy*cm in drainage, both $p < 0.001$) [52]. Although reports on the efficacy of DLR in CT-guided tumor ablation are scarce, dose reduction by DLR may be particularly beneficial in ablation therapies as they generally require higher radiation doses than those in biopsy or drainage [53]. For instance, DLR might be advantageous in CT-guided renal cryoablation, where the radiation dose can be high because of multiple needle insertions and repeated CT scans for iceball monitoring [54–56]. The doses may be reduced with DLR while maintaining the image quality required for implementing the procedure (Fig. 2).

Other deep learning applications for image quality improvement in CT-guided procedures include reduced needle artifacts and the generation of virtual contrast-enhanced images. Cao et al. reported a deep learning model for metal artifact reduction in CT-guided interventional oncology procedures [57]. They scanned CT images with various cryoprobe configurations in a phantom and created images with and without probe artifacts using intensity thresholding. Probes with and without artifacts were segmented and inserted into patient images to simulate procedural images, and a U-net-type model was then trained for metal artifact reduction using these simulated images. When applied to CT images obtained during actual renal cryoablation, this model significantly improved the visual assessment scores by 34–46% for overall image quality, iceball conspicuity, needle tip visualization, target region confidence, and metal artifacts. Pinnock et al. reported a deep learning method using a conditional GAN to generate multi-phase synthetic contrast-enhanced CT images for interventional procedures [58]. They trained the models using pre-procedural CT data from 34 patients undergoing renal cryoablation and demonstrated the feasibility of generating virtual contrast-enhanced CT images of various phases from non-contrast CT. Notably, their model could perform virtual contrast enhancement even on images containing cryoprobes and an iceball that were not present in the training data. Although such a method may have the potential to enable better visualization of target lesions, as in contrast-enhanced CT, without actually administering contrast media during ablation therapies, whether the quality of the synthetic images is sufficiently high and reliable for clinical use remains to be validated.

Additionally, deep learning has the potential to improve the image quality of distal subtraction angiography (DSA) during transcatheter procedures. An inherent limitation of DSA is the presence of misregistration artifacts caused by misalignment between the mask and contrast-enhanced images. To overcome this limitation, some investigators explored the use of deep learning to generate synthetic DSA images without masks, initially focusing on cerebral

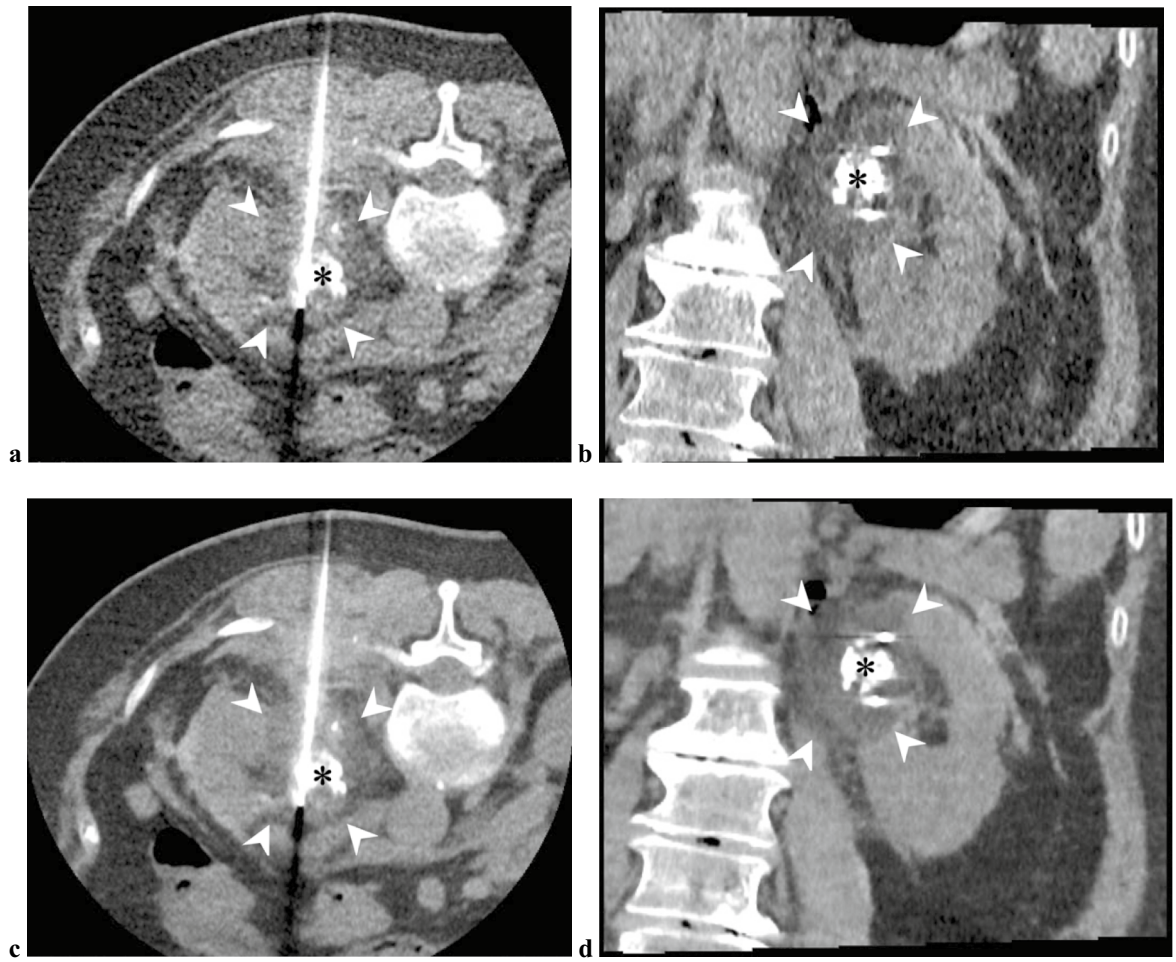

Fig. 2 CT images immediately after freezing in a cryoablation procedure for a left renal cell carcinoma, with the patient in the prone position (**a**, **c**: axial section; **b**, **d**: coronal section). **(a, b)** Images reconstructed from low-dose raw data using a hybrid iterative reconstruction algorithm (AIDR 3D; Canon Medical Systems, Otawara, Japan). **(c, d)** Images reconstructed from the same raw data using a deep learning reconstruction algorithm (AiCE; Canon Medical Systems). The tumor (asterisks), which appears to have a high density owing to prior transarterial lipiodol marking, is encompassed within the low-density iceball (arrowheads). The images reconstructed using the deep learning reconstruction algorithm provide less image noise and a more conspicuous iceball contour

angiography [59, 60]. Ueda et al. developed a deep learning-based model to generate cerebral DSA-like images using a conditional GAN trained with pairs of dynamic angiograms and DSA without misregistration [59]. The quantitative evaluation showed a sufficiently high coincidence between the DSA-like images generated by the model and the original DSA. Furthermore, a visual evaluation conducted using a test dataset comprising misregistered images demonstrated that the DSA-like images achieved similar or better scores than those by the original DSA. More recently, Crabb et al. reported a similar approach to generate deep learning-based DSA-like images of the hepatic and splenic arteries [61]. This method can potentially address the issue of misregistration artifacts caused by patient motion, respiratory movement of organs, and intestinal peristalsis, which obscure the visualization of target tumors and feeding vessels in transcatheter cancer treatments, such as TACE for HCC. However, further investigations are necessary before its use in clinical practice, including whether deep learning-based DSA ensures sufficient visualization of tumor staining.

Prediction of treatment outcomes

Predicting treatment outcomes is crucial for selecting appropriate strategies for each patient. Therefore, investigators have pursued AI-based models that provide accurate prognostic predictions after intervention. The development of AI-based predictive models includes multiple steps, such as data extraction, key feature selection, and model construction. The data entered into the model can be clinical, radiological, or both. Clinical data can include patient demographics,

laboratory findings, tumor characteristics, and procedure-related data such as ablation parameters. Radiological data can be obtained from radiomics analysis or manual image evaluation. The outcomes predicted from these data include treatment response, survival, or complications. Machine learning can be partially or comprehensively used to construct predictive models [62]. When using clinical or handcrafted radiological features as inputs, machine learning can be employed for feature selection, model building, or both; however, standard statistical methods may also be used for these purposes. In radiomics, machine learning contributes to image processing, feature selection, and final model building. Furthermore, deep learning allows the skipping of multiple steps and direct processing of image inputs to predict outputs [62]. When incorporating clinical and radiomics features into a model, they can be entered simultaneously into models using machine learning. Alternatively, the clinical and radiomics models can be built separately and later combined using methods, such as nomograms, to develop an integrated model.

AI-based predictive models have been frequently reported for the treatment of liver tumors, particularly HCC. Hsieh et al. previously reviewed studies published until 2022 on machine learning and radiomics for the prognosis prediction of TACE and ablation for HCC [62]. In their review, the models for TACE showed an area under the curve (AUC) of 0.81–0.99 in predicting tumor response (responders [complete or partial response] vs. non-responders [stable or progressive disease], mainly based on modified Response Evaluation Criteria in Solid Tumors). The models for ablative therapies showed C-indexes of 0.72–0.73 in predicting progression-free or recurrence-free survivals. In addition, two meta-analyses on the radiomics-based prediction of outcomes after TACE for HCC have been published. The earlier one by Feng et al. included six studies published until October 2022, and showed a pooled sensitivity and specificity of 0.90 and 0.81, respectively, for predicting tumor response [63]. The latter study by Wang et al. included 24 studies published until July 2023 and showed that the radiomics-clinical model achieved C-indexes of 0.88 and 0.80 for predicting treatment response and survival status, respectively [64]. Moreover, Mirza-Aghazadeh-Attari et al. conducted a meta-analysis of studies published until May 2023 to evaluate the radiomics-based prediction of tumor response after radioembolization for liver tumor, showing a pooled sensitivity and specificity of 0.84 and 0.87, respectively [65]. Notably, studies using machine learning techniques to predict the outcomes of liver tumor treatments have been successively published, even after these meta-analyses. The most recent studies published in 2023 or later are summarized in Tables 1 and 2, excluding those included in the aforementioned meta-analyses. In these studies, the models for TACE provided AUC of 0.70–0.96 and 0.80–0.93 for predicting overall survival and tumor response, respectively (Table 1) [66–78]. The models for ablative therapies provided an AUC of 0.83–0.98 for the prediction of local tumor control (Table 2) [79–83].

While most studies on AI-based outcome prediction thus far have been conducted on liver tumors, a few reports have shown similar results for lung tumor ablation [85–87]. Crombé et al. investigated a radiomics model to predict local tumor progression (LTP) following RFA of colorectal cancer lung metastases [85]. Conventional machine learning algorithms were trained using radiomic features extracted from the ablation zone segmented on early follow-up CT, and the best model showed a moderate AUC of 0.72. They suggested that the performance of their radiomics model might have been limited by the capture of inflammation, intra-alveolar hemorrhage, cavitation, and fistulization during complicated procedures.

As described above, AI-based predictive models have demonstrated moderate-to-high predictive performance. Such AI-based prognostication may be useful for supporting treatment decision-making [88–90]. However, the study results should be interpreted with caution in terms of reproducibility, given the diversity of the proposed models. The details of the method vary widely among studies regarding input features (clinical, radiomics, or both), imaging modality, image processing method, and machine learning algorithms [62–65]. Furthermore, the performance of these models has not always been evaluated using external test cohorts. Hence, the superiority of any particular algorithm is not evident and requires further investigation.

Detection of post-treatment recurrence

AI-based techniques for lesion detection in radiological images have been studied extensively. For example, there are a number of reports on the AI-based detection of pulmonsary nodules on CT [91], and such AI models have been clinically implemented. Consequently, AI is expected to be useful in detecting recurrent lesions after image-guided therapies. Early detection of local recurrences on follow-up images is important to promptly consider a secondary strategy, including reintervention. However, detecting local recurrence on follow-up images can be more complicated than detecting de novo lesions because of post-treatment changes in the region of interest. In image-guided tumor ablation, LTP is identified as a nodular enhanced focus within or adjacent to the ablation zone [92, 93]. To detect early LTP, a small focus needs to be extracted from the treatment area, where radiological changes due to reactive inflammation and scarring are usually observed. Despite this difficulty, some investigators have used AI to facilitate LTP detection on follow-up

Table 1 Most recent studies using machine learning to predict outcomes of transarterial treatments for hepatocellular carcinoma

Author, Year	Treatment	No. of participants[a]	Outcomes predicted	Input	Methods		Best model performance
					Feature selection	Model construction	
Liu Y 2024 [66]	cTACE	110 (Internal testing by five-fold cross-validation)	TR[b] (mRECIST)	Clinical data MRI (radiomics)	cML	DL cML Nomogram[c]	AUC: 0.87
Peng G 2024 [67]	cTACE	Training: 248 Test (internal): 107	EHM	Clinical data MRI (radiomics)	cML	cML Nomogram[c]	C-index: 0.83 AUC: 0.83/0.82/0.89/0.95/0.93 for 1/2/3/4/5 yr EHM probability
Wang Q 2024 [68]	TACE with ablation	Training: 172 Test (internal): 75	RFS	Clinical data	cML	Nomogram	C-index: 0.64 AUC: 0.69/0.72/0.75 for 1/3/5 yr RFS
Yang C 2024 [69]	cTACE	Training: 77 Test (internal): 34	OS	Clinical data MRI (radiomics)	cML	cML	C-index: 0.80 AUC: 0.83[d]
Zhang L 2024 [70]	cTACE	Training: 181 Test (external): 186	TR[b] (mRECIST)	Clinical data CT (handcrafted features)	Standard statistical method	cML	AUC: 0.80
Sun Z 2024 [71]	TACE	Training: 241 Test (internal): 60	OS	Clinical data CT (radiomics)	DL cML	DL cML	C-index: 0.88 AUC 0.96 for 3 yr OS
Chen Y 2024 [72]	TACE	Training: 1,075 Test (internal): 269 Test (external): 414	OS	Clinical data	Standard statistical method	DL	C-index: 0.70 AUC: 0.77/0.73/0.70 for 1/3/5 yr OS
Zhang X 2024 [73]	DEB-TACE	Training: 86 Test (internal): 22	TR[b] (mRECIST)	Clinical data CT (Radiomics)	cML	cML Nomogram[c]	AUC: 0.93
Liu W 2024 [74)]	TACE HAIC	Training: 1,700 Test (internal): 428 Test (external): 200	OS	Clinical data	cML	cML	AUC: 0.81/0.74/0.70/0.79 for 1/2/3/5 yr OS
İnce O 2023 [75]	cTACE DEB-TACE	188 Training/test (internal) = 7/3	TR[b] (EASL)	Clinical data MRI (radiomics)	cML	cML	AUC: 0.91
Li J 2023 [76]	DEB-TACE	Training: 201 Test (internal): 87	ALFD	Clinical data	cML	Nomogram	AUC: 0.88
Liang Y 2023 [77]	Postoperative TACE	274 Training/ test (internal) = 8/2	OS RFS	Clinical data	NA	cML	AUC: 0.91/0.94/0.95 for 1/2/3 yr OS, 0.81/0.85/0.83 for 1/2/3 yr RFS
Ma J 2023 [78]	TACE with lenvatinib	Training: 88 Test (internal): 37	TR[b] (mRECIST)	Clinical data	cML	cML	AUC: 0.91

[a]The definitions of data set terms varied across studies. To avoid ambiguity due to inconsistent terminology, the names of data sets in the table are listed according to the following definitions [84], regardless of the terms used in the original papers: i) Training: a data set used for initial learning to determine model parameters, ii) Validation: a data set used for parameter tuning and model refinement, iii) Test: a data set used to

Table 1 (continued)

evaluate the final model performance. A test set can be either internal (split from the same pool as the training set) or external (unrelated to the training and internal testing sets, differing from these temporally or geographically)

[b]Responders showed complete or partial response, and non-responders exhibited stable or progressive disease

[c]Nomogram integrated clinical and radiomics models

[d]A mean value of multiple time-dependent AUC values across 6–54 months from enrollment

TACE = transarterial chemoembolization, *cTACE* = conventional TACE, *DEB-TACE* = drug eluting beads TACE, *HAIC* = hepatic arterial infusion chemotherapy, *TR* = treatment response, *mRECIST* = modified Response Evaluation Criteria in Solid Tumors, *EASL* = European Association for the Study of the Liver criteria, *EHM* = extrahepatic metastasis, *RFS* = recurrence free survival, *OS* = overall survival, *ALFD* = acute liver function deterioration, *MRI* = magnetic resonance imaging, *CT* = computed tomography, *cML* = conventional machine learning, *DL* = deep learning, *NA* = not applicable, *AUC* = area under the curve

Table 2 Most recent studies using machine learning to predict outcomes of ablation therapies for liver tumors

Author, Year	Treatment	No. of participants[a]	Outcomes predicted	Input	Methods		Best model performance
					Feature selection	Model construction	
Hamed AA 2024 [79]	RFA for HCC	111 Training/Test (internal) = 7/3	RFS	Clinical data	NA	cML	AUC: 0.80 for 1 yr RFS
Sato M 2023 [80]	RFA for HCC	Training: 1,422 Validation: 178 Test (internal): 178	OS	Clinical data	NA	DL	C-index: 0.69
Ren H 2023 [81]	MWA for HCC	Training: 607 Test (external): 299	LTP	Clinical data	cML	cML	AUC: 0.90 for LTP within 2 yrs
Shahveranova A 2023 [82]	MWA for CRLM	42[b]	LTP	Clinical data MRI (radiomics)	cML	cML	AUC: 0.98 for LTP within 6 months
Tabari A 2023 [83]	RFA or MWA for HCC[c]	97 Training/validation/ test (internal) = 6/2/2	Pathological response[d]	Clinical data MRI (radiomics)	cML	cML	AUC: 0.83

[a]The definitions of data set terms varied across studies. To avoid ambiguity due to inconsistent terminology, the names of data sets in the table are listed according to the following definitions [84], regardless of the terms used in the original papers: i) Training: a data set used for initial learning to determine model parameters, ii) Validation: a data set used for parameter tuning and model refinement, iii) Test: a data set used to evaluate the final model performance. A test set can be either internal (split from the same pool as the training set) or external (unrelated to the training and internal testing sets, differing from these temporally or geographically)

[b]No internal or external testing was performed

[c]RFA or MWA were performed as bridge to liver transplant

[d]Histopathology was assessed at the time of liver transplant

RFA = radiofrequency ablation, *MWA* = microwave ablation, *HCC* = hepatocellular carcinoma, *CRLM* = colorectal carcinoma liver metastases, *RFS* = recurrence free survival, *OS* = overall survival, *LTP* = local tumor progression, *MRI* = magnetic resonance imaging, *NA* = not applicable, *cML* = conventional machine learning, *DL* = deep learning, *AUC* = area under the curve

imaging. Yin et al. investigated the efficacy of machine learning-based radiomics analysis for detecting LTP on follow-up contrast-enhanced CT after thermal ablation of HCC and metastatic liver tumors [94]. Radiomics features were extracted from the region of interest, including the ablation zone and surrounding liver parenchyma on follow-up CT images, and models were trained using the selected features. The best-performing model achieved an accuracy of 92.7% and an AUC of 0.97 for detecting LTP. Lim et al. developed a deep learning method to detect LTP after RFA or MWA for HCC using follow-up CT images [95]. Their deep CNN model used 3D patches extracted from arterial-phase CT images to detect LTP. The model performance on test datasets demonstrated an accuracy of 97.6% and an AUC of 0.99 in detecting LTP.

Current issues and future directions

Research has explored a wide variety of AI models for various tasks in interventional oncology procedures. As AI technology advances, more AI-based methods will be developed. Similar to AI, extended reality (virtual, augmented, and mixed reality) and robotics have gained attention as cutting-edge technologies that can be useful in interventional oncology [26, 96]. The integration of AI with these technologies may further enhance advanced image-guided cancer treatment [97]. The potential benefits of introducing AI include not only improved workflow and treatment outcomes, but also a reduction in radiation exposure to patients and physicians—an inherent issue in image-guided interventions. Although its significance in interventional oncology procedures remains to be validated, the evolution of X-ray fluoroscopy and DSA technologies by AI-based image processing may contribute to greatly reduced intraoperative radiation doses [98, 99].

However, most AI-based methods discussed in this review are still in the research phase, and few have been implemented in clinical practice. Investigators have utilized various algorithms to develop and test AI models, making objective evaluation and impartial comparison of model performance across studies difficult, even among those aiming for similar tasks. Therefore, the real-world performance and clinical reliability of AI-based methods must be interpreted carefully. Additionally, the relatively small datasets available in the field of interventional radiology compared with those in diagnostic radiology could be a limitation in the development of AI models [24]. The establishment and widespread clinical use of highly reliable AI models across various areas and institutions are still uncertain. The Cardiovascular and Interventional Radiological Society of Europe outlines several conditions for the widespread use of AI in daily clinical practice, including ensuring sufficient accuracy and reliability, seamless integration with procedural workflows, and meeting regulatory requirements [100]. They also highlighted the need to integrate computer science and AI knowledge into education and training because it might become as important for interventional radiologists as knowledge in biostatistics. Moreover, when employing AI-based technologies, we need to recognize fairness issues in AI, which are caused by potential biases from data, algorithms, and AI clinician/patient interactions [101].

In conclusion, AI has the potential to enhance various aspects of interventional oncology practice, from treatment planning to post-treatment follow-up. For AI technologies to be widely adopted in interventional oncology procedures, further investigations of their reliability and clinical utility are necessary. Despite this challenge, various AI technologies will be incorporated into interventional oncology in the near future, because of the rapid research progress in this field.

Acknowledgements ChatGPT, DeepL, and Grammarly were used for English editing in the manuscript preparation process, and the validity of all text was thoroughly confirmed by the authors. We would like to thank Editage (www.editage.jp) for the final English editing.

Author contributions All authors contributed to the conceptualization of this review. Y.M. conducted the literature search and review. The first draft of the manuscript was prepared by Y.M., and all the co-authors critically revised the manuscript. The final version of the manuscript was approved for submission by all authors.

Funding This study was not supported by any funding.

Declarations

Conflict of interest Y.M. received a grant and lecturer fee from Canon Medical Systems outside the submitted work. The other authors have no relevant financial or non-financial interests to disclose.

Ethical approval.

Ethical approval was not required for this review.

References

1. Yanagawa M, Ito R, Nozaki T, Fujioka T, Yamada A, Fujita S, et al. New trend in artificial intelligence-based assistive technology for thoracic imaging. Radiol Med. 2023;128:1236–49.
2. Fujima N, Kamagata K, Ueda D, Fujita S, Fushimi Y, Yanagawa M, et al. Current state of artificial intelligence in clinical applications for head and neck MR imaging. Magn Reson Med Sci. 2023;22:401–14.
3. Tatsugami F, Nakaura T, Yanagawa M, Fujita S, Kamagata K, Ito R, et al. Recent advances in artificial intelligence for cardiac CT: enhancing diagnosis and prognosis prediction. Diagn Interv Imaging. 2023;104:521–8.
4. Yamada A, Kamagata K, Hirata K, Ito R, Nakaura T, Ueda D, et al. Clinical applications of artificial intelligence in liver imaging. Radiol Med. 2023;128:655–67.
5. Hirata K, Kamagata K, Ueda D, Yanagawa M, Kawamura M, Nakaura T, et al. From FDG and beyond: the evolving potential of nuclear medicine. Ann Nucl Med. 2023;37:583–95.
6. Hirata K, Sugimori H, Fujima N, Toyonaga T, Kudo K. Artificial intelligence for nuclear medicine in oncology. Ann Nucl Med. 2022;36:123–32.
7. Toda N, Hashimoto M, Iwabuchi Y, Nagasaka M, Takeshita R, Yamada M, et al. Validation of deep learning-based computer-aided detection software use for interpretation of pulmonary

abnormalities on chest radiographs and examination of factors that influence readers' performance and final diagnosis. Jpn J Radiol. 2023;41:38–44.
8. Uematsu T, Nakashima K, Harada TL, Nasu H, Igarashi T. Comparisons between artificial intelligence computer-aided detection synthesized mammograms and digital mammograms when used alone and in combination with tomosynthesis images in a virtual screening setting. Jpn J Radiol. 2023;41:63–70.
9. Ishihara M, Shiiba M, Maruno H, Kato M, Ohmoto-Sekine Y, Antoine C, et al. Detection of intracranial aneurysms using deep learning-based CAD system: usefulness of the scores of CNN's final layer for distinguishing between aneurysm and infundibular dilatation. Jpn J Radiol. 2023;41:131–41.
10. Nakao T, Hanaoka S, Nomura Y, Hayashi N, Abe O. Anomaly detection in chest 18F-FDG PET/CT by Bayesian deep learning. Jpn J Radiol. 2022;40:730–9.
11. Lv E, Liu W, Wen P, Kang X. Classification of benign and malignant lung nodules based on deep convolutional network feature extraction. J Healthc Eng. 2021;2021:8769652.
12. Goto M, Sakai K, Toyama Y, Nakai Y, Yamada K. Use of a deep learning algorithm for non-mass enhancement on breast MRI: comparison with radiologists' interpretations at various levels. Jpn J Radiol. 2023;41:1094–103.
13. Ozaki J, Fujioka T, Yamaga E, Hayashi A, Kujiraoka Y, Imokawa T, et al. Deep learning method with a convolutional neural network for image classification of normal and metastatic axillary lymph nodes on breast ultrasonography. Jpn J Radiol. 2022;40:814–22.
14. Gao R, Zhao S, Aishanjiang K, Cai H, Wei T, Zhang Y, et al. Deep learning for differential diagnosis of malignant hepatic tumors based on multi-phase contrast-enhanced CT and clinical data. J Hematol Oncol. 2021;14:154.
15. Tanaka T, Huang Y, Marukawa Y, Tsuboi Y, Masaoka Y, Kojima K, et al. Differentiation of small (≤ 4 cm) renal masses on multi-phase contrast-enhanced CT by deep learning. Am J Roentgenol. 2020;214:605–12.
16. Oshima S, Fushimi Y, Miyake KK, Nakajima S, Sakata A, Okuchi S, et al. Denoising approach with deep learning-based reconstruction for neuromelanin-sensitive MRI: image quality and diagnostic performance. Jpn J Radiol. 2023;41:1216–25.
17. Hamabuchi N, Ohno Y, Kimata H, Ito Y, Fujii K, Akino N, et al. Effectiveness of deep learning reconstruction on standard to ultra-low-dose high-definition chest CT images. Jpn J Radiol. 2023;41:1373–88.
18. Hosoi R, Yasaka K, Mizuki M, Yamaguchi H, Miyo R, Hamada A, et al. Deep learning reconstruction with single-energy metal artifact reduction in pelvic computed tomography for patients with metal hip prostheses. Jpn J Radiol. 2023;41:863–71.
19. Yasaka K, Akai H, Sugawara H, Tajima T, Akahane M, Yoshioka N, et al. Impact of deep learning reconstruction on intracranial 1.5 T magnetic resonance angiography. Jpn J Radiol. 2022;40(5):476–83.
20. Kaga T, Noda Y, Mori T, Kawai N, Miyoshi T, Hyodo F, et al. Unenhanced abdominal low-dose CT reconstructed with deep learning-based image reconstruction: image quality and anatomical structure depiction. Jpn J Radiol. 2022;40:703–11.
21. Kitahara H, Nagatani Y, Otani H, Nakayama R, Kida Y, Sonoda A, et al. A novel strategy to develop deep learning for image super-resolution using original ultra-high-resolution computed tomography images of lung as training dataset. Jpn J Radiol. 2022;40:38–47.
22. Kawamura M, Kamomae T, Yanagawa M, Kamagata K, Fujita S, Ueda D, et al. Revolutionizing radiation therapy: the role of AI in clinical practice. J Radiat Res. 2024;65:1–9.
23. Chapiro J, Allen B, Abajian A, Wood B, Kothary N, Daye D, et al. Proceedings from the Society of Interventional Radiology Foundation Research Consensus Panel on artificial intelligence in interventional radiology: from code to bedside. J Vasc Interv Radiol. 2022;33:1113–20.
24. Seah J, Boeken T, Sapoval M, Goh GS. Prime time for artificial intelligence in interventional radiology. Cardiovasc Intervent Radiol. 2022;45:283–9.
25. Gurgitano M, Angileri SA, Rodà GM, Liguori A, Pandolfi M, Ierardi AM, et al. Interventional radiology ex-machina: impact of artificial intelligence on practice. Radiol Med. 2021;126:998–1006.
26. von Ende E, Ryan S, Crain MA, Makary MS. Artificial intelligence, augmented reality, and virtual reality advances and applications in interventional radiology. Diagnostics (Basel). 2023;13:892.
27. Fite EL, Makary MS. Transarterial chemoembolization treatment paradigms for hepatocellular carcinoma. Cancers. 2024;16:2430.
28. Higashihara H, Kimura Y, Ono Y, Tanaka K, Tomiyama N. Effective utilization of conventional transarterial chemoembolization and drug-eluting bead transarterial chemoembolization in hepatocellular carcinoma: a guide to proper usage. Interv Radiol. 2023. https://doi.org/10.22575/interventionalradiology.2023-0009.
29. Matsui Y, Iguchi T, Tomita K, Uka M, Sakurai J, Gobara H, et al. Radiofrequency ablation for stage I non-small cell lung cancer: an updated review of literature from the last decade. Interv Radiol. 2020;5:43–9.
30. Matsui Y, Tomita K, Uka M, Umakoshi N, Kawabata T, Munetomo K, et al. Up-to-date evidence on image-guided thermal ablation for metastatic lung tumors: a review. Jpn J Radiol. 2022;40:1024–34.
31. Tomita K, Matsui Y, Uka M, Umakoshi N, Kawabata T, Munetomo K, et al. Evidence on percutaneous radiofrequency and microwave ablation for liver metastases over the last decade. Jpn J Radiol. 2022;40:1035–45.
32. Fujimori M, Yamanaka T, Sugino Y, Matsushita N, Sakuma H. Percutaneous image-guided thermal ablation for renal cell carcinoma. Interv Radiol. 2020;5:32–42.
33. Meek RD, Lungren MP, Gichoya JW. Machine learning for the interventional radiologist. Am J Roentgenol. 2019;213:782–4.
34. Hwang JH, Seo JW, Kim JH, Park S, Kim YJ, Kim KG. Comparison between deep learning and conventional machine learning in classifying iliofemoral deep venous thrombosis upon CT venography. Diagnostics (Basel). 2022;12:274.
35. Fusco R, Granata V, Grazzini G, Pradella S, Borgheresi A, Bruno A, et al. Radiomics in medical imaging: pitfalls and challenges in clinical management. Jpn J Radiol. 2022;40:919–29.
36. He K, Liu X, Shahzad R, Reimer R, Thiele F, Niehoff J, et al. Advanced deep learning approach to automatically segment malignant tumors and ablation zone in the liver with contrast-enhanced CT. Front Oncol. 2021;11: 669437.
37. Bilic P, Christ P, Li HB, Vorontsov E, Ben-Cohen A, Kaissis G, et al. The liver tumor segmentation benchmark (LiTS). Med Image Anal. 2023;84: 102680.
38. Fang X, Xu S, Wood BJ, Yan P. Deep learning-based liver segmentation for fusion-guided intervention. Int J Comput Assist Radiol Surg. 2020;15:963–72.
39. Mahmoodian N, Chakrabarty S, Georgiades M, Pech M, Hoeschen C. Multi-class tissue segmentation of CT images using an ensemble deep learning method. Conf Proc IEEE Eng Med Biol Soc. 2023;2023:1–4.
40. Müller D, Soto-Rey I, Kramer F. Towards a guideline for evaluation metrics in medical image segmentation. BMC Res Notes. 2022;15:210.
41. Taha AA, Hanbury A. Metrics for evaluating 3D medical image segmentation: analysis, selection, and tool. BMC Med Imaging. 2015;15:29.

42. Zhou C, Zhao X, Zhao L, Liu J, Chen Z, Fang S. Deep learning-based CT imaging in the diagnosis of treatment effect of pulmonary nodules and radiofrequency ablation. Comput Intell Neurosci. 2022;2022:7326537.
43. Malpani R, Petty CW, Yang J, Bhatt N, Zeevi T, Chockalingam V, et al. Quantitative automated segmentation of lipiodol deposits on cone-beam CT imaging acquired during transarterial chemoembolization for liver tumors: a deep learning approach. J Vasc Interv Radiol. 2022;33:324-32.e2.
44. Chaichana A, Frey EC, Teyateeti A, Rhoongsittichai K, Tocharoenchai C, Pusuwan P, et al. Automated segmentation of lung, liver, and liver tumors from Tc-99m MAA SPECT/CT images for Y-90 radioembolization using convolutional neural networks. Med Phys. 2021;48:7877–90.
45. Lin Z-Y, Li G-L, Chen J, Chen Z-W, Chen Y-P, Lin S-Z. Effect of heat sink on the recurrence of small malignant hepatic tumors after radiofrequency ablation. J Cancer Res Ther. 2016;12:C153–8.
46. Iguchi T, Matsui Y, Hiraki T. Overcoming cold-sink effect of blood flow during thermal ablation of central renal cancer. Diagn Interv Imaging. 2022;103:497–8.
47. Keshavamurthy KN, Eickhoff C, Ziv E. Pre-operative lung ablation prediction using deep learning. Eur Radiol. 2024. https://doi.org/10.1007/s00330-024-10767-8.
48. Moreira P, Tuncali K, Tempany C, Tokuda J. AI-based isotherm prediction for focal cryoablation of prostate cancer. Acad Radiol. 2023;30:S14-20.
49. Haste P, Tann M, Persohn S, LaRoche T, Aaron V, Mauxion T, et al. Correlation of technetium-99m macroaggregated albumin and yttrium-90 glass microsphere biodistribution in hepatocellular carcinoma: a retrospective review of pretreatment single photon emission CT and post-treatment positron emission tomography/CT. J Vasc Interv Radiol. 2017;28:722-30.e1.
50. Plachouris D, Tzolas I, Gatos I, Papadimitroulas P, Spyridonidis T, Apostolopoulos D, et al. A deep-learning-based prediction model for the biodistribution of 90 Y microspheres in liver radioembolization. Med Phys. 2021;48:7427–38.
51. Tanahashi Y, Kubota K, Nomura T, Ikeda T, Kutsuna M, Funayama S, et al. Improved vascular depiction and image quality through deep learning reconstruction of CT hepatic arteriography during transcatheter arterial chemoembolization. Jpn J Radiol. 2024. https://doi.org/10.1007/s11604-024-01614-3.
52. Matsumoto T, Endo K, Yamamoto S, Suda S, Tomita K, Kamei S, et al. Dose length product and outcome of CT fluoroscopy-guided interventions using a new 320-detector row CT scanner with deep-learning reconstruction and new bow-tie filter. Br J Radiol. 2022;95:20211159.
53. Kloeckner R, dos Santos DP, Schneider J, Kara L, Dueber C, Pitton MB. Radiation exposure in CT-guided interventions. Eur J Radiol. 2013;82:2253–7.
54. Levesque VM, Shyn PB, Tuncali K, Tatli S, Nawfel RD, Olubiyi O, et al. Radiation dose during CT-guided percutaneous cryoablation of renal tumors: effect of a dose reduction protocol. Eur J Radiol. 2015;84:2218–21.
55. Matsui Y, Hiraki T, Gobara H, Iguchi T, Fujiwara H, Kawabata T, et al. Radiation exposure of interventional radiologists during computed tomography fluoroscopy-guided renal cryoablation and lung radiofrequency ablation: direct measurement in a clinical setting. Cardiovasc Intervent Radiol. 2016;39:894–901.
56. Seki Y, Miyazaki M, Fukushima Y, Ando M, Tsushima Y. Radiation exposure of interventional radiologists during computed tomography fluoroscopy-guided percutaneous cryoablation. Interv Radiol (Higashimatsuyama). 2020;5:67–73.
57. Cao W, Parvinian A, Adamo D, Welch B, Callstrom M, Ren L, et al. Deep convolutional-neural-network-based metal artifact reduction for CT-guided interventional oncology procedures (MARIO). Med Phys. 2024;51:4231–42.
58. Pinnock MA, Hu Y, Bandula S, Barratt DC. Time conditioning for arbitrary contrast phase generation in interventional computed tomography. Phys Med Biol. 2024;69: 115010.
59. Ueda D, Katayama Y, Yamamoto A, Ichinose T, Arima H, Watanabe Y, et al. Deep learning-based angiogram generation model for cerebral angiography without misregistration artifacts. Radiology. 2021;299:675–81.
60. Gao Y, Song Y, Yin X, Wu W, Zhang L, Chen Y, et al. Deep learning-based digital subtraction angiography image generation. Int J Comput Assist Radiol Surg. 2019;14:1775–84.
61. Crabb BT, Hamrick F, Richards T, Eiswirth P, Noo F, Hsiao A, et al. Deep learning subtraction angiography: improved generalizability with transfer learning. J Vasc Interv Radiol. 2023;34:409-19.e2.
62. Hsieh C, Laguna A, Ikeda I, Maxwell AWP, Chapiro J, Nadolski G, et al. Using machine learning to predict response to image-guided therapies for hepatocellular carcinoma. Radiology. 2023;309: e222891.
63. Feng L, Chen Q, Huang L, Long L. Radiomics features of computed tomography and magnetic resonance imaging for predicting response to transarterial chemoembolization in hepatocellular carcinoma: a meta-analysis. Front Oncol. 2023;13:1194200.
64. Wang Y, Li M, Zhang Z, Gao M, Zhao L. Application of radiomics in the efficacy evaluation of transarterial chemoembolization for hepatocellular carcinoma: a systematic review and meta-analysis. Acad Radiol. 2024;31:273–85.
65. Mirza-Aghazadeh-Attari M, Srinivas T, Kamireddy A, Kim A, Weiss CR. Radiomics features extracted from pre- and postprocedural imaging in early prediction of treatment response in patients undergoing transarterial radioembolization of hepatic lesions: a systematic review, meta-analysis, and quality appraisal study. J Am Coll Radiol. 2024;21:740–51.
66. Liu Y, Liu Z, Li X, Zhou W, Lin L, Chen X. Non-invasive assessment of response to transcatheter arterial chemoembolization for hepatocellular carcinoma with the deep neural networks-based radiomics nomogram. Acta Radiol. 2024;65:535–45.
67. Peng G, Cao X, Huang X, Zhou X. Radiomics and machine learning based on preoperative MRI for predicting extrahepatic metastasis in hepatocellular carcinoma patients treated with transarterial chemoembolization. Eur J Radiol Open. 2024;12: 100551.
68. Wang Q, Sheng S, Xiong Y, Han M, Jin R, Hu C. Machine learning-based model for predicting tumor recurrence after interventional therapy in HBV-related hepatocellular carcinoma patients with low preoperative platelet-albumin-bilirubin score. Front Immunol. 2024;15:1409443.
69. Yang C, Yang H-C, Luo Y-G, Li F-T, Cong T-H, Li Y-J, et al. Predicting survival using whole-liver MRI radiomics in patients with hepatocellular carcinoma after TACE refractoriness. Cardiovasc Intervent Radiol. 2024;47:964–77.
70. Zhang L, Jin Z, Li C, He Z, Zhang B, Chen Q, et al. An interpretable machine learning model based on contrast-enhanced CT parameters for predicting treatment response to conventional transarterial chemoembolization in patients with hepatocellular carcinoma. Radiol Med. 2024;129:353–67.
71. Sun Z, Li X, Liang H, Shi Z, Ren H. A Deep learning model combining multimodal factors to predict the overall survival of transarterial chemoembolization. J Hepatocell Carcinoma. 2024;11:385–97.
72. Chen Y, Shi Y, Wang R, Wang X, Lin Q, Huang Y, et al. Development and validation of deep learning model for intermediate-stage hepatocellular carcinoma survival with transarterial

chemoembolization (MC-hccAI 002): a retrospective, multicenter, cohort study. J Cancer. 2024;15:2066–73.
73. Zhang X, He Z, Zhang Y, Kong J. Prediction of initial objective response to drug-eluting beads transcatheter arterial chemoembolization for hepatocellular carcinoma using CT radiomics-based machine learning model. Front Pharmacol. 2024;15:1315732.
74. Liu W, Wei R, Chen J, Li Y, Pang H, Zhang W, et al. Prognosis prediction and risk stratification of transarterial chemoembolization or intraarterial chemotherapy for unresectable hepatocellular carcinoma based on machine learning. Eur Radiol. 2024;34:5094–107.
75. İnce O, Önder H, Gençtürk M, Cebeci H, Golzarian J, Young S. Machine learning models in prediction of treatment response after chemoembolization with MRI clinicoradiomics features. Cardiovasc Intervent Radiol. 2023;46:1732–42.
76. Li J, Zhang Y, Ye H, Hu L, Li X, Li Y, et al. Machine learning-based development of nomogram for hepatocellular carcinoma to predict acute liver function deterioration after drug-eluting beads transarterial chemoembolization. Acad Radiol. 2023;30:S40-52.
77. Liang Y, Wang Z, Peng Y, Dai Z, Lai C, Qiu Y, et al. Development of ensemble learning models for prognosis of hepatocellular carcinoma patients underwent postoperative adjuvant transarterial chemoembolization. Front Oncol. 2023;13:1169102.
78. Ma J, Bo Z, Zhao Z, Yang J, Yang Y, Li H, et al. Machine learning to predict the response to lenvatinib combined with transarterial chemoembolization for unresectable hepatocellular carcinoma. Cancers. 2023;15:625.
79. Hamed AA, Muhammed A, Abdelbary EAM, Elsharkawy RM, Ali MA. Can machine learning predict favorable outcome after radiofrequency ablation of hepatocellular carcinoma? JCO Clin Cancer Inform. 2024;8: e2300216.
80. Sato M, Moriyama M, Fukumoto T, Yamada T, Wake T, Nakagomi R, et al. Development of a transformer model for predicting the prognosis of patients with hepatocellular carcinoma after radiofrequency ablation. Hepatol Int. 2023;18:131–7.
81. Ren H, An C, Fu W, Wu J, Yao W, Yu J, et al. Prediction of local tumor progression after microwave ablation for early-stage hepatocellular carcinoma with machine learning. J Cancer Res Ther. 2023;19:978–87.
82. Shahveranova A, Balli HT, Aikimbaev K, Piskin FC, Sozutok S, Yucel SP. Prediction of local tumor progression after microwave ablation in colorectal carcinoma liver metastases patients by MRI radiomics and clinical characteristics-based combined model: preliminary results. Cardiovasc Intervent Radiol. 2023;46:713–25.
83. Tabari A, D'Amore B, Cox M, Brito S, Gee MS, Wehrenberg-Klee E, et al. Machine learning-based radiomic features on pre-ablation MRI as predictors of pathologic response in patients with hepatocellular carcinoma who underwent hepatic transplant. Cancers. 2023;15:2058.
84. Walston SL, Seki H, Takita H, Mitsuyama Y, Sato S, Hagiwara A, et al. Data set terminology of deep learning in medicine: a historical review and recommendation. Jpn J Radiol. 2024. https://doi.org/10.1007/s11604-024-01608-1.
85. Crombé A, Palussière J, Catena V, Cazayus M, Fonck M, Béchade D, et al. Radiofrequency ablation of lung metastases of colorectal cancer: could early radiomics analysis of the ablation zone help detect local tumor progression? Br J Radiol. 2023;96:20201371.
86. Markich R, Palussière J, Catena V, Cazayus M, Fonck M, Bechade D, et al. Radiomics complements clinical, radiological, and technical features to assess local control of colorectal cancer lung metastases treated with radiofrequency ablation. Eur Radiol. 2021;31:8302–14.
87. Xu S, Qi J, Li B, Bie Z-X, Li Y-M, Li X-G. Risk prediction of pleural effusion in lung malignancy patients treated with CT-guided percutaneous microwave ablation: a nomogram and artificial neural network model. Int J Hyperthermia. 2021;38:220–8.
88. Wang D-D, Zhang J-F, Zhang L-H, Niu M, Jiang H-J, Jia F-C, et al. Clinical-radiomics predictors to identify the suitability of transarterial chemoembolization treatment in intermediate-stage hepatocellular carcinoma: a multicenter study. Hepatobiliary Pancreat Dis Int. 2023;22:594–604.
89. Mo A, Velten C, Jiang JM, Tang J, Ohri N, Kalnicki S, et al. Improving adjuvant liver-directed treatment recommendations for unresectable hepatocellular carcinoma: an artificial intelligence-based decision-making tool. JCO Clin Cancer Inform. 2022;6: e2200024.
90. Choi GH, Yun J, Choi J, Lee D, Shim JH, Lee HC, et al. Development of machine learning-based clinical decision support system for hepatocellular carcinoma. Sci Rep. 2020;10:14855.
91. Chassagnon G, De Margerie-Mellon C, Vakalopoulou M, Marini R, Hoang-Thi T-N, Revel M-P, et al. Artificial intelligence in lung cancer: current applications and perspectives. Jpn J Radiol. 2023;41:235–44.
92. Umakoshi N, Iguchi T, Matsui Y, Tomita K, Uka M, Kawabata T, et al. Renal cryoablation combined with prior transcatheter arterial embolization in non-dialysis patients with stage 4 or 5 chronic kidney disease: a retrospective study. Jpn J Radiol. 2023;41:1007–14.
93. Uka M, Iguchi T, Okawa N, Matsui Y, Tomita K, Umakoshi N. Percutaneous cryoablation for clinical T3a renal cell carcinoma (< 7 cm) with segmental vein involvement or perinephric fat invasion based on preoperative evaluation of high - resolution multidetector computed tomography scan. Jpn J Radiol. 2022;40:1201–9.
94. Yin Y, de Haas RJ, Alves N, Pennings JP, Ruiter SJS, Kwee TC, et al. Machine learning-based radiomic analysis and growth visualization for ablation site recurrence diagnosis in follow-up CT. Abdom Radiol (NY). 2024;49:1122–31.
95. Lim S, Shin Y, Lee YH. Arterial enhancing local tumor progression detection on CT images using convolutional neural network after hepatocellular carcinoma ablation: a preliminary study. Sci Rep. 2022;12:1754.
96. Matsui Y, Kamegawa T, Tomita K, Uka M, Umakoshi N, Kawabata T, et al. Robotic systems in interventional oncology: a narrative review of the current status. Int J Clin Oncol. 2024;29:81–8.
97. Arapi V, Hardt-Stremayr A, Weiss S, Steinbrener J. Bridging the simulation-to-real gap for AI-based needle and target detection in robot-assisted ultrasound-guided interventions. Eur Radiol Exp. 2023;7:30.
98. Bang JY, Hough M, Hawes RH, Varadarajulu S. Use of artificial intelligence to reduce radiation exposure at fluoroscopy-guided endoscopic procedures. Am J Gastroenterol. 2020;115:555–61.
99. Zhao H, Xu Z, Chen L, Wu L, Cui Z, Ma J, et al. Large-scale pre-trained frame generative model enables real-time low-dose DSA imaging: an AI system development and multi-center validation study. Med. 2024. https://doi.org/10.1016/j.medj.2024.07.025.
100. Najafi A, Cazzato RL, Meyer BC, Pereira PL, Alberich A, López A, et al. CIRSE position paper on artificial intelligence in interventional radiology. Cardiovasc Intervent Radiol. 2023;46:1303–7.
101. Ueda D, Kakinuma T, Fujita S, Kamagata K, Fushimi Y, Ito R, et al. Fairness of artificial intelligence in healthcare: review and recommendations. Jpn J Radiol. 2024;42:3–15.

Authors and Affiliations

Yusuke Matsui[1] · Daiju Ueda[2] · Shohei Fujita[3] · Yasutaka Fushimi[4] · Takahiro Tsuboyama[5] · Koji Kamagata[6] · Rintaro Ito[7] · Masahiro Yanagawa[8] · Akira Yamada[9] · Mariko Kawamura[7] · Takeshi Nakaura[10] · Noriyuki Fujima[11] · Taiki Nozaki[12] · Fuminari Tatsugami[13] · Tomoyuki Fujioka[14] · Kenji Hirata[15] · Shinji Naganawa[7]

✉ Yusuke Matsui
y-matsui@okayama-u.ac.jp

1 Department of Radiology, Faculty of Medicine, Dentistry and Pharmaceutical Sciences, Okayama University, 2-5-1 Shikata-Cho, Kita-Ku, Okayama 700-8558, Japan

2 Department of Artificial Intelligence, Graduate School of Medicine, Osaka Metropolitan University, Abeno-Ku, Osaka, Japan

3 Department of Radiology, Graduate School of Medicine and Faculty of Medicine, The University of Tokyo, Bunkyo-Ku, Tokyo, Japan

4 Department of Diagnostic Imaging and Nuclear Medicine, Kyoto University Graduate School of Medicine, Sakyoku, Kyoto, Japan

5 Department of Radiology, Kobe University Graduate School of Medicine, Chuo-Ku, Kobe, Japan

6 Department of Radiology, Juntendo University Graduate School of Medicine, Bunkyo-Ku, Tokyo, Japan

7 Department of Radiology, Nagoya University Graduate School of Medicine, Showa-Ku, Nagoya, Japan

8 Department of Radiology, Osaka University Graduate School of Medicine, Suita-City, Osaka, Japan

9 Medical Data Science Course, Shinshu University School of Medicine, Matsumoto, Nagano, Japan

10 Department of Diagnostic Radiology, Kumamoto University Graduate School of Medicine, Chuo-Ku, Kumamoto, Japan

11 Department of Diagnostic and Interventional Radiology, Hokkaido University Hospital, Kita-Ku, Sapporo, Japan

12 Department of Radiology, Keio University School of Medicine, Shinjuku-Ku, Tokyo, Japan

13 Department of Diagnostic Radiology, Hiroshima University, Minami-Ku, Hiroshima, Japan

14 Department of Diagnostic Radiology, Tokyo Medical and Dental University, Bunkyo-Ku, Tokyo, Japan

15 Department of Diagnostic Imaging, Graduate School of Medicine, Hokkaido University, Kita-Ku, Sapporo, Japan